Induced Draft Forced Cooling Process for Anode Baking Furnace

Chao Liu[1], Chaodong Liu[2], Shanhong Zhou[3] and Wei Hu[4]
1. Senior Engineer
2, 3. Professor Level Senior Engineers
Shenyang Aluminum and Magnesium Engineering & Research Institute (SAMI), Shenyang, China
1. PhD Candidate
Northeastern University - School of Metallurgy, Shenyang, China
4. Manager
Beijing Autosky Science & Technology, Beijing, China
Corresponding author: neu_liuch@126.com
https://doi.org/10.71659/icsoba2025-el012

Abstract

In the context of the continuous large scale evolution of the anode baking furnace, the drawbacks of the traditional blowing draft forced cooling process (BD-FCP) have become increasingly prominent. This traditional method, which involves blowing hot air into the workshop, not only leads to a continuous rise in the production environment temperature, severely deteriorating the working conditions for workers, but also poses a significant threat to the stable and normal operation of equipment. To address these issues, this study proposes replacing the traditional BD-FCP with an induced draft forced cooling process (ID-FCP). In the new process, the hot air after heat exchange is efficiently evacuated from the workshop through the induced draft system for subsequent heat recovery. In the current work, advanced numerical simulation technology is utilized to conduct a comprehensive and in-depth comparative analysis between the two cooling processes. The calculation results indicate that the cooling rate of anodes in the ID-FCP is comparable to that in the BD-FCP. Additionally, the flue gas exhaust temperature of the induced-draft system can reach 150–230 °C, which satisfies the temperature requirements for heat recovery. Therefore, the ID-FCP can fully meet the cooling requirements of baked anodes, significantly reduce the ambient temperature in the workshop, and successfully recover waste heat during the baking forced cooling stage. This new process comprehensively contributes to energy consumption reduction in anode production, representing a promising technological innovation in this field.

Keywords: Anode for aluminium, Anode baking furnace, Combustion control system, Blowing draft forced cooling process, Induced draft forced cooling process

1. Introduction

The open-type ring baking furnace (BF) is the core production equipment for the high-temperature modification of green anodes in the carbon industry. The anode baking process is executed by the furnace combustion control system (FCCS) according to a pre-defined temperature ramp profile. Based on the control phases of FCCS over anode temperature evolution, the baking cycle is divided into four sequential stages: preheating phase, heating phase, natural cooling phase, and forced cooling phase.

The anodes in the furnace section are heated to approximately 1100 °C after the preheating and heating phases, then their physical and chemical properties will meet the requirements for electrolytic production. Prior to the discharge of high-temperature anodes from the furnace section, their temperature must be reduced to a reasonable level. To optimize production

efficiency and economic viability, this temperature is set as the minimum value between the maximum permissible operating temperature of the discharge equipment and the minimum threshold to prevent anode oxidation. The temperature reduction is achieved through the natural and forced cooling phases.

During the natural cooling phase, cold air from the workshop is blown into the flue channels via blowing ramps, reducing the temperature of high-temperature anodes to approximately 600 °C. Meanwhile, the preheated cooling air is directed to the furnace sections in the heating phase for combustion support, enabling partial heat recovery. In the forced cooling phase, blowing ramps are also used to introduce cold workshop air into the flue channels for cooling. Unlike the natural cooling phase, the peephole covers above the flue channels in the forced cooling area are opened, allowing cold air to discharge heat from the flue channels through the open peepholes into the workshop. This lowers the anode temperature below 300 °C [1], making the anodes ready for discharge.

2. Problems of Traditional Forced Cooling Processes

During the forced cooling phase, cold air from the baking workshop is blown into the flue channels by blowing ramps. After heat exchange, the air flows out through the furnace-top peepholes and dissipates into the workshop, transferring substantial heat from the furnace to the workshop environment and raising the ambient temperature. With the continuous development of larger-scale baking furnaces, the physical size of baking workshops has increased, exacerbating the problem of excessive ambient temperatures. In some sites, peak temperatures can exceed 70 °C in summer, not only deteriorating the working environment for operators but also causing malfunctions in equipment such as the cranes and combustion control systems, which disrupts normal production. This has become a significant challenge plaguing the baking workshop operations.

From the perspective of heat balance [2], before anode blocks enter the cooling stage, heat stored in the furnace, heat carried away by packing materials, and heat carried away by baked anodes account for 80 % of the total heat expenditure. Upon entering the natural cooling zone, a portion of the heat re-enters the system through preheated air, while another portion dissipates through the furnace surface. In the forced cooling furnace sections, the majority of the heat is transferred into the baking workshop via forced cooling, with the remaining heat retained in the refractory materials, anode blocks, and packing materials. Typically, the temperature in natural cooling furnace sections drops from approximately 1100 to 700 °C, and that in forced cooling furnace sections decreases from 700 to around 300 °C. Therefore, it can be estimated that about 20 % of the total heat input, equivalent to approximately 1.5 GJ/t of anode, is carried into the baking workshop by the cooling air in the forced cooling zone. Based on the heat balance, the heat dissipation from the entire baking furnace surface is estimated to account for around 20 % of the heat input. This analysis reveals that the excessively high temperature in the baking furnace workshop is caused not only by heat dissipation from the furnace surface but also by the release of hot air in the forced cooling zone.

To address the above issues, the study proposes a process route that replaces blowing ramps with induced-draft ramps during the forced cooling phase. Cold air is drawn into the flue channels through peepholes to cool the anodes, and the heated air is discharged from the workshop via an induced-draft system for heat recovery. The induced-draft system comprises an induced draft ramp, insulated conveying pipelines, and a medium-low temperature flue gas waste heat recovery system. The induced draft ramp shares structural similarity with the currently employed blowing ramps, albeit with induced draft fans substituting for blowers. The induced draft ramp traverses along the baking furnace floor in conjunction with the firing system operation. One end of the induced draft ramp adjacent to the ring main functions as its smoke exhaust port, which is

connected to the flue gas conveying pipelines distributed around the workshop. The connection mode is analogous to that between the exhaust ramp and the ring main. The extracted medium-low temperature flue gas may be directed to the flue gas waste heat recovery system for residual heat utilisation, or discharged directly into the baking flue gas purification system. This approach not only reduces the ambient temperature inside the workshop but also comprehensively lowers the baking energy consumption of anodes. This technology has currently applied for a Chinese invention patent and has been applied in actual production.

3. Numerical Simulation Study on Forced Cooling Process of Baking Furnace

Numerical simulation technology has been widely applied to optimize the structure and processes of anode baking furnaces, with its effectiveness verified in engineering applications [3–7]. To theoretically analyze the application effects of different forced cooling processes, this study conducts a comparative analysis using numerical simulation by fluent, laying a theoretical foundation for the internal balance of the baking furnace combustion control system and the production practice of ID-FCP.

3.1 Physical Model

Large open-type baking furnaces offer significant advantages over small traditional ones in terms of anode quality, product energy consumption, and investment cost, representing the development trend of carbon anode baking and the preferred solution for new projects. Therefore, this study selects the design parameters of a large operational baking furnace as model parameters to establish a physical model, considering real structural parameters such as flue tie bricks. To effectively control the number of grids while balancing computational accuracy, the furnace sections from the 4C to 7C stages of a single combustion control system (corresponding to four furnace sections) are selected as the research object. A symmetrical boundary is applied by taking half of the flue channels and half of the pits for analysis. Under idealized conditions, the influence of edge flue channels is excluded, so the research object is assumed to be the middle pits. Additionally, the physical model of this study is shown in Figure 1.

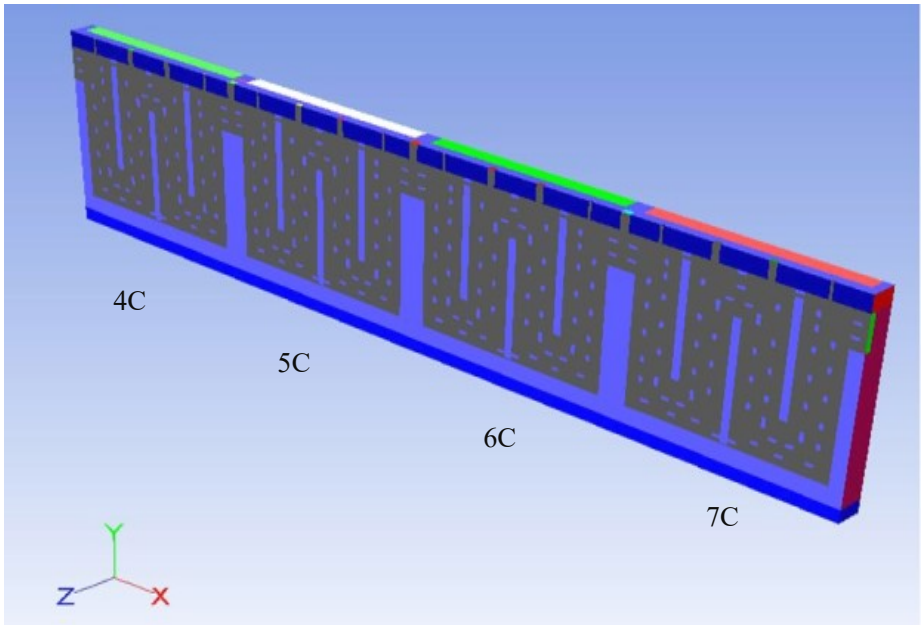

Figure 1. Physical model for numerical simulation of an open-type BF from 4C to 7C stages.

3.2 Mathematical Models

The development of ID-FCP technology for open-type baking furnaces essentially involves studying unsteady flow and heat transfer in a three-dimensional structure. During numerical simulation, the main mathematical models include the continuity equation, energy conservation equation, and momentum conservation equation.

3.2.1 Mass Conservation

Mass conservation is a fundamental law of nature: for any open system, the mass of matter entering and leaving the system is equal to the mass changing within the system. The continuity equation describes the basic law of mass conservation in fluid mechanics, revealing the relationship between the rate of changing of fluid density with time and the divergence of the fluid velocity vector. Based on mass conservation in the control volume of the open-type BF, the differential form of the three-dimensional unsteady continuity equation is derived as:

$$\frac{\partial \rho}{\partial t} + \frac{\partial (\rho u)}{\partial x} + \frac{\partial (\rho v)}{\partial y} + \frac{\partial (\rho w)}{\partial z} = 0 \quad (1)$$

where:

ρ	fluid density, kg/m^3
t	time, s
u, v and w	components of the velocity vector in the x, y and z directions, m/s

Using the divergence operator ∇ and velocity vector $\boldsymbol{u}$, the continuity equation can be simplified to:

$$\frac{\partial \rho}{\partial t} + \nabla \cdot (\rho \boldsymbol{u}) = 0 \quad (2)$$

3.2.2 Momentum Conservation

The momentum conservation equation is an application of Newton's second law in fluid mechanics, stating that the rate of increase in momentum of a fluid per unit volume in a given direction equals the net inflow of momentum in that direction plus the sum of external forces acting in that direction. Its differential form is:

$$\frac{\partial \rho u_i}{\partial t} + \nabla \cdot (\rho \boldsymbol{u} u_i) = \nabla \cdot (\mu \nabla u_i) - \frac{\partial p}{\partial x_i} + S_T \quad (3)$$

where:

ρ	fluid density, kg/m^3
$\boldsymbol{u}$	fluid velocity vector, m/s
p	pressure, Pa
μ	dynamic viscosity, Pa·s
t	time, s
S_T	generalized source term, kg/m^2·s^2

3.2.3 Energy Conservation

Energy manifests in diverse forms throughout nature, for any open system, however, the total energy influx and efflux are conserved with the energy variation within the system. In studies of simple heat transfer problems, energy conservation is primarily described by the heat conservation

equation. For the computational processes involved in this model, the differential form of heat conservation for three-dimensional unsteady-state conditions without internal heat sources is employed:

$$\frac{\partial}{\partial t}(\rho h) + \nabla \cdot (\rho \boldsymbol{u} h) = \nabla \cdot \left(\frac{\lambda}{C_P} \nabla h\right) - p \nabla \cdot \boldsymbol{u} \quad (4)$$

where:

ρ	fluid density, kg/m^3
$\boldsymbol{u}$	fluid velocity vector, m/s
p	pressure, Pa
h	specific enthalpy, J/kg
λ	thermal conductivity, W/m·K
C_p	specific heat capacity, J/kg·K
t	time, s

3.3 Boundary Conditions

3.3.1 Material Physical Properties

During the numerical simulation, the main physical properties include the specific gravity, thermal conductivity, and specific heat capacity of materials involved in the model. To improve the accuracy of repeated iterative calculations, the temperature-dependent property data from the literature [8] were fitted.

3.3.2 Heat Transfer Boundaries

Heat transfer in the computational domain encompasses heat dissipation from the castable at the top of flue channels and the packing material at the top of pits to the external environment, involving complex heat transfer processes of conduction, convection, and radiation. The overall heat transfer coefficient documented in the literature [8] is employed to calculate the heat loss from furnace walls to the ambient. Additionally, internal surfaces are set as adiabatic boundaries to disregard internal heat conduction.

3.3.3 Flow Boundary Conditions

Flow boundaries were determined by integrating on-site measurements from a large-scale open-type baking furnace. For forced cooling racks:

- BD-FCP: Specified as mass flow inlets.
- ID-FCP: Defined as pressure outlets.

Peephole configurations were referenced against operational data from the target furnace. Specifically for BD-FCP in the 4C-stage section, the upstream two peepholes are kept open during the blowing phase, while all other peepholes remain closed.

4. Calculation Results and Analysis

First, the operational conditions of the traditional BD-FCP were calculated. The anode temperature within the 4C-7C chamber of the traditional BD-FCP was measured utilizing thermocouples. Through comparative analysis of the calculated data and test data, the accuracy of the numerical simulation model was verified. On this basis, the feasibility and theoretical process scheme of ID-FCP were explored.

4.1 Numerical Simulation of BD-FCP

Using the operating parameters of the natural cooling racks and forced cooling racks in BD-FCP as input conditions, the current process was calculated and analyzed. Table 1 lists the comparison between the final temperatures of anodes in the 4C–7C furnace sections before removal, as obtained from numerical simulation and test results. The data in the table shows that the error between the numerical results and the actual test results of the anode final cooling temperatures is within 5 %, meeting the requirements for calculation accuracy.

Table 1. Calculated and tested final temperatures of anodes (BD-FCP).

Zone of Anode in Baking Furnace	4C	5C	6C	7C
Calculated Final Temperature (°C)	524	428	332	269
Tested Final Temperature (°C)	527	425	323	279
Calculation Error	0.61 %	0.74 %	2.80 %	3.58 %

Figures 2 and 3 illustrate the main flow of cooling air and the corresponding anode cooling conditions in the furnace sections. As shown in the calculated contour plots, the calculated results of anodes final temperature are below 300 °C, so the traditional BD-FCP demonstrates favourable cooling performance. Notably, the areas corresponding to the three upstream peepholes in Section 5C and one downstream peephole in Section 6C exhibit relatively high temperatures before anode removal.

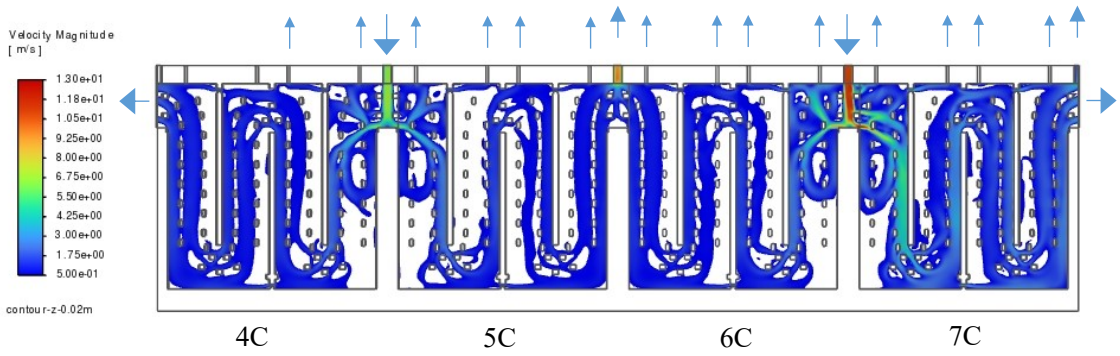

Figure 2. Final velocity contour of cooling air in sections 4C–7C (BD-FCP).

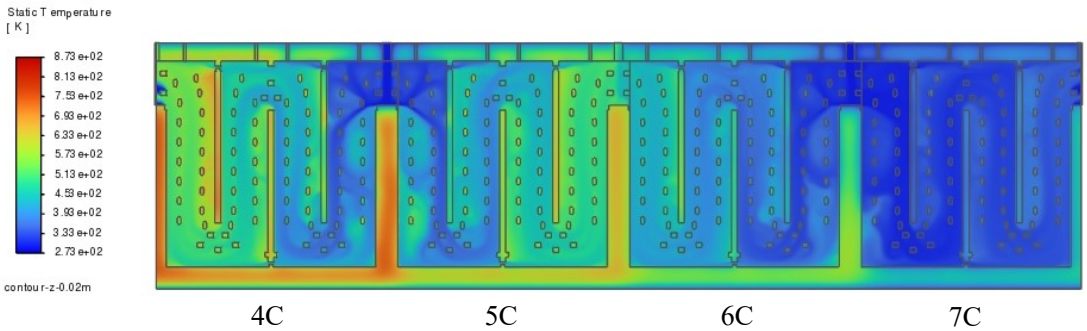

Figure 3. Final cooling temperature contour of anodes in sections 4C–7C (BD-FCP).

4.2 Numerical Simulation of ID-FCP

Owing to modifications in the cooling process route, the following optimizations were implemented for the ID-FCP scheme prior to computations:

1) In BD-FCP, the opening of peepholes adjacent to the blowing rack induces substantial cooling air overflow. For ID-FCP, to prevent compromising the cooling capacity of the forced cooling rack on distant flues, one peephole on each lateral side adjacent to the ID-FCP rack is sealed.
2) In comparison with BD-FCP, ID-FCP causes a greater proportion of cooling air injected into flues by the natural cooling rack to be extracted by the ID-FCP rack. To ensure an adequate supply of preheated air to the heating zone, all peepholes in the 4C stage and one peephole in the adjacent 5C stage are shut.

Based on the aforementioned process adjustments, through numerical simulation and iterative refinement of calculation results, the final cooling temperatures of anodes before removal at various stages are tabulated in Table 2.

Table 2. Calculated and tested final temperatures of anodes (ID-FCP).

Zone of Anode in Baking Furnace	4C	5C	6C	7C
Calculated Final Temperature (°C)	536	398	335	265
Tested Final Temperature (°C)	527	425	323	279
Test-Calculation Deviation* (°C)	-9	+27	-12	+14

* "+" indicates that the cooling temperature exceeds the test requirement (overcooling), while "-" indicates that the cooling temperature is lower than the test requirement (undercooling).

As indicated by Table 2, the final cooling temperature of anodes at the 7C stage under ID-FCP is lower than the test requirement, while other stages show minor overcooling and undercooling within acceptable limits. These results, valid within the model error margin, confirm the feasibility of implementing ID-FCP in industrial baking processes.

Figures 4 and 5 depict the main cooling air flow and anode temperature contours of ID-FCP, highlighting distinct differences from BD-FCP. The negative pressure generated by the induced draft rack diverts a larger proportion of cooling air from natural cooling racks into the 5C-stage flues, necessitating adjustments to peephole closure to maintain preheated air supply. Notably, the high-temperature zones in 5C and 6C stages shift rearward, with overall average temperatures lower than BD-FCP, fully meeting production specifications.

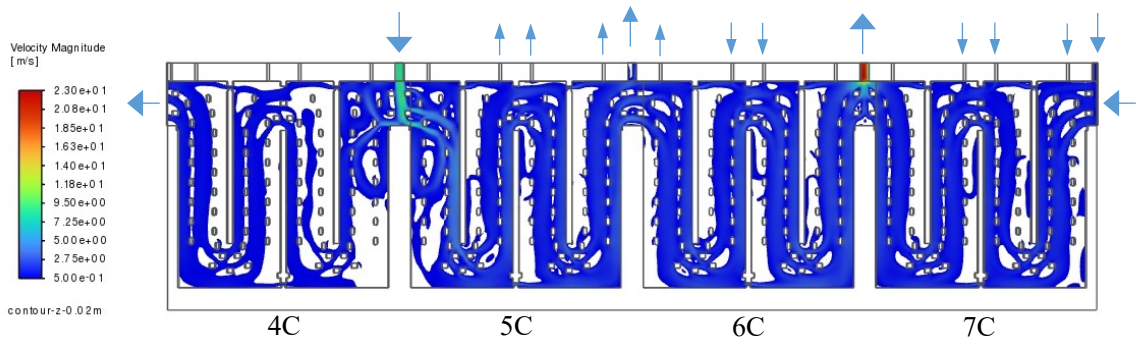

Figure 4. Final velocity contour of cooling air in sections 4C–7C (ID-FCP).

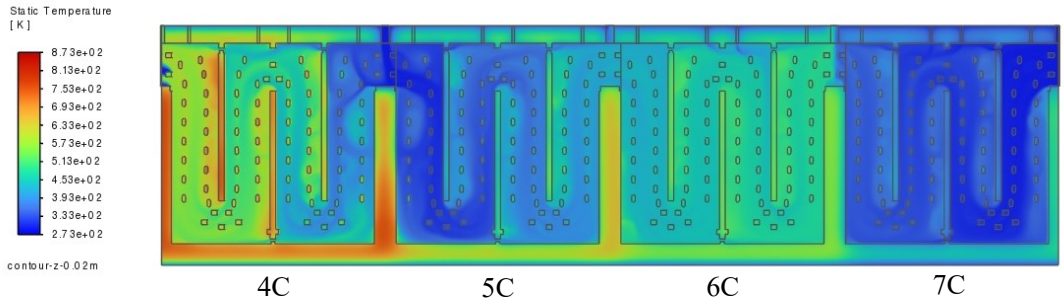

Figure 5. Final cooling temperature tontour of anodes in sections 4C–7C (ID-FCP).

4.3 Comparative Analysis of Theoretical Calculation Results for Both Processes

4.3.1 Cooling Rate

The cooling rate significantly influences anode cracking and overall quality. Theoretical calculations yield the cooling rate profiles of anodes within the charge box under BD-FCP and ID-FCP for sections 4C–7C, as shown in Figures 6(a–d). As indicated by Figure 6, ID-FCP exhibits slightly lower cooling rates than traditional BD-FCP at the 4C and 7C stages, while notable differences emerge at 5C and 6C: ID-FCP demonstrates a faster cooling rate at 5C, while BD-FCP shows a higher cooling rate at 6C. This trend aligns with the rearward shift of high-temperature zones observed in Figures 3 and 5. Overall, the maximum cooling rates of the two processes are comparable, with primary differences in cooling performance at 5C and 6C sections—these differences do not significantly affect the final temperature at the 7C stage.

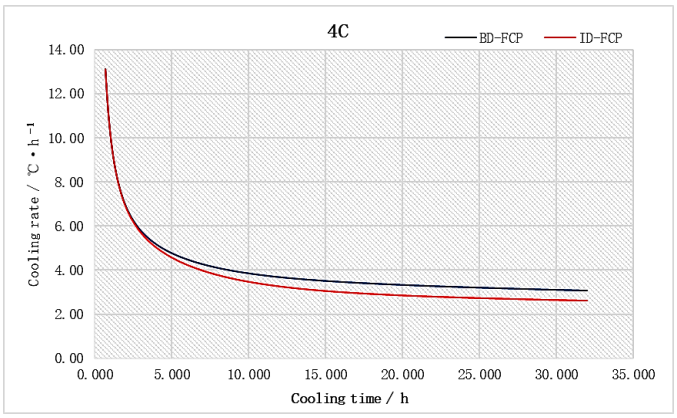

(a)

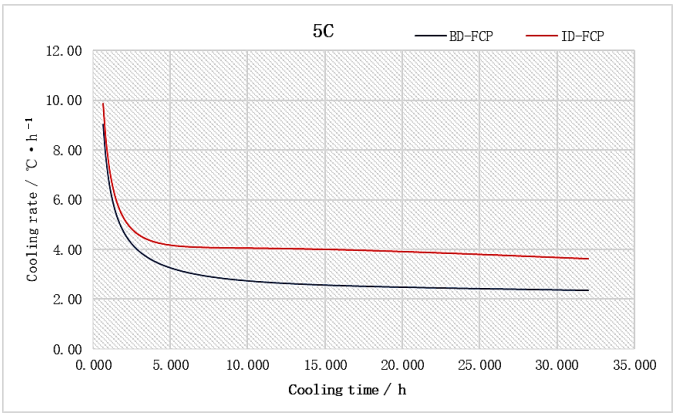

(b)

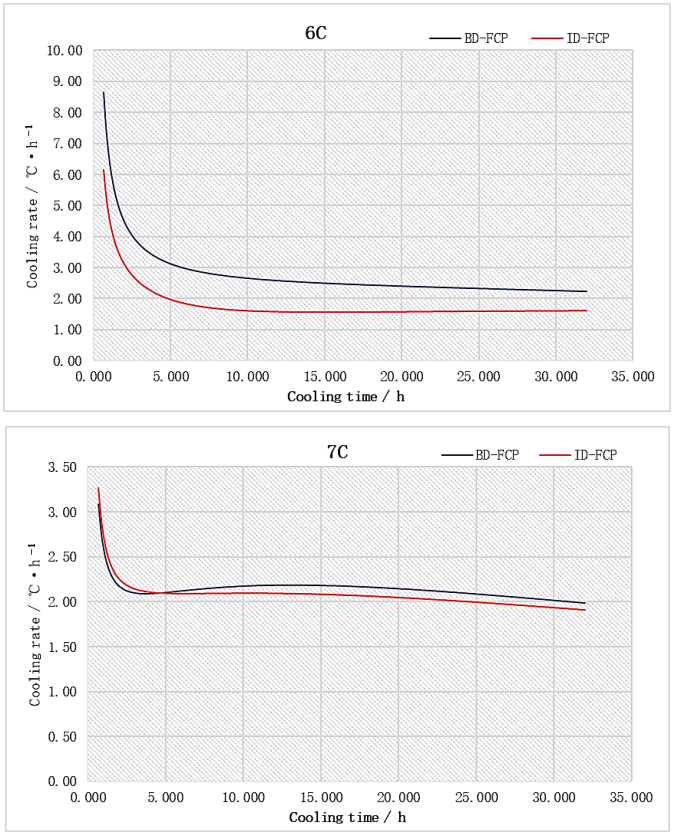

(c)

(d)

Figure 6. Anode cooling rates (°C/h) of two forced cooling processes (Black curve = BD-FCP, Red curve = ID-FCP) at different stages, over a 35-h period. (a): 4C stage, (b): 5C stage, (c): 6C stage, (d): 7C stage.

4.3.2 Pressure Loss

Theoretical calculations show that the ID-FCP requires greater extraction force from the induced draft fan. The pressure loss across the cross-wall peepholes between the induced draft fan outlet and 7C–8C sections approaches 200 Pa, whereas that between the blowing fan inlet and 7C–8C sections in BD-FCP is only 40 Pa. For natural cooling racks, pressure loss across cross-wall peepholes between the fan inlet and 3C–4C sections remains similar under both processes, within 10 Pa. Considering frictional resistance in pipelines, ID-FCP demands significantly higher power input than BD-FCP.

4.3.3 Exhaust Gas Temperature

ID-FCP enables waste heat recovery during the intensive cooling phase. The exhaust gas temperature must meet the minimum threshold for low-temperature waste heat recovery; higher temperatures enhance economic benefits of heat recovery, making exhaust temperature a key performance indicator for ID-FCP.

The calculated results indicate that during the 32 h cooling cycle, the maximum induced draft temperature reaches 230 °C, gradually decreasing to 150 °C over time. While this meets the lower temperature limit for low-grade heat recovery, it highlights the low exergy quality of waste gases in ID-FCP. Optimal recovery strategies include:

- Stage-wise heat recovery of medium–low temperature flue gases by temperature segments;

- Utilization for hot water production or winter heating in carbon block warehouses in northern regions.

5. Conclusions

This study establishes a numerical simulation model for the forced cooling phase of an open-loop ring baking furnace, validated by test data for calculation accuracy. Through theoretical calculations and comparative analysis of BD-FCP and ID-FCP using numerical simulation, the results show:

1. The ID-FCP combustion control system can reduce the final anode cooling temperature to below 300 °C. Throughout the 4C–7C stages, the maximum anode cooling rate does not exceed BD-FCP computational data, meeting production process requirements and confirming ID-FCP feasibility.

2. The ID-FCP exhaust gas temperature exceeds 150 °C, satisfying the lower limit for low-temperature waste heat recovery. This enables comprehensive reduction of baking energy consumption and addresses the high-temperature issue in baking workshops during summer.

6. References

1. Wang Limin, Analysis of cracking phenomenon in carbon anodes during baking process, *Light Metals* 2010, (09): 47–51 (in Chinese).
2. Wang Nan and Liu Zhaodong, Heat balance testing and analysis for the large open baking furnace, *Light Metals* 2016, (04): 39–43 (in Chinese).
3. Li Hao, Numerical simulation and optimization of open anode baking furnace, Master's Thesis, Central South University, Hunan, China, 2010.
4. Liu Zhaodong, Cui Yinhe, and Zhou Shanhong, Three-dimensional numerical simulation model of anode baking furnace process, *Light Metals* 2013, 55–59 (in Chinese).
5. Zhou Guanchen et al., Numerical simulation of oxygen-enriched combustion in open ring anode baking furnace, *Journal of Materials and Metallurgy*, Vol. 21, No. 3 (2022), 172–177.
6. Han Li et al., Simulation energy-saving analysis and application of new carbon baking furnace, *Light Metals* 2024, 35–40 (in Chinese).
7. Abdul Raouf Tajik et al., The effects of flue-wall design modifications on combustion and flow characteristics of an aluminum anode baking furnace—CFD modeling, *Applied Energy*, Vol. 230 (2018), 207–219.
8. Mei Chi and Zhou Ping, *Design Handbook of Nonferrous Metal Furnaces*, Changsha: Central South University Press, 2018, 103 pages.